

Conference code: MI101
Title of conference: Physics of Medical Imaging

This work has not been submitted for publication or presentation elsewhere.

Generalized Filtered Back-projection for Digital Breast Tomosynthesis Reconstruction

Klaus Erhard^a, Michael Grass^a, Sebastian Hitziger^b,
Armin Iske^b, and Tim Nielsen^a

^aPhilips Research Europe – Hamburg, Germany

^bUniversity of Hamburg, Germany

1 Purpose

Filtered back-projection (FBP) has been commonly used as an efficient and robust reconstruction technique in tomographic X-ray imaging during the last decades. For limited angle tomography acquisitions such as digital breast tomosynthesis, however, standard FBP reconstruction algorithms provide poor results and give rise to image artifacts due to the limited angular range and the coarse angular sampling. Therefore, iterative algorithms are often used in digital breast tomosynthesis since they potentially yield a reconstructed image that is in better accordance with the measured data. In this work, a generalized FBP algorithm is presented, which uses the filtered projection data of all acquired views for back-projection along one direction in order to compute an image that is similar to an iteratively calculated one. The proposed method requires the computation of geometry-dependent filter kernels that provide an efficient reconstruction algorithm with an accuracy comparable to iterative techniques, which will be demonstrated on simulated breast tomosynthesis data.

2 Methods

While FBP algorithms provide fast and accurate image reconstruction in tomographic X-Ray imaging whenever the source trajectory is complete and sufficiently many projections are acquired [4], they perform worse on limited angle tomographic data where both the trajectory is incomplete and the sampling is coarse. In digital breast tomosynthesis, for example, typical examination protocols acquire only 10 - 30 X-ray projections over a limited angular range of 15° - 60° [2]. Here, a common FBP image reconstruction suffers from severe artefacts such as the loss of the average value and edge sharpening along the source trajectory. These artefacts can be weakened with the use of iterative reconstruction techniques since these kind of algorithms successively update the reconstructed image in order to reduce the mismatch between measured projection data and the reprojections generated from the current image.

Motivation of the filter design A similar reconstruction quality as for example with an ART algorithm cannot be achieved with a view-by-view filtering of the projection data in standard FBP reconstruction since the update step of ART implicitly involves information from all projection angles prior to back-projecting from one single view. To mimic this feature of iterative reconstruction algorithms cross-view projection filtering has to be enabled within the FBP framework. Therefore, a more general filtered backprojection is introduced by

$$x = BFy, \tag{1}$$

with image x , measured projection data

$$y = (y_1, \dots, y_N)^T, \tag{2}$$

Send correspondence to Klaus Erhard, e-mail: klaus.erhard@philips.com

filter matrix

$$F = \begin{pmatrix} F_{11} & \dots & F_{1N} \\ \vdots & \ddots & \vdots \\ F_{N1} & \dots & F_{NN} \end{pmatrix} \quad (3)$$

and the back-projection operator

$$B = \frac{1}{N} (B_1, \dots, B_N) . \quad (4)$$

Here, y_i denotes the measured data for the source position i , i.e. $Px = y$ with the projection operator

$$P = (P_1, \dots, P_N)^T , \quad (5)$$

defined via the projection operators P_i for each view position i . Note, that in contrast to standard FBP algorithms, the filter matrices F_{ij} , acting on the measured data y_j and contributing to the filtered view i prior to back-projecting from source position i , are non-zero for the proposed generalized FBP method.

Computation of an image x^\dagger that is consistent with the measured data can be achieved with the knowledge of the generalized inverse P^+ of the projection operator P via

$$x^\dagger = P^+ y . \quad (6)$$

However, direct computation of the generalized inverse is not feasible due to the complexity of P and therefore iterative methods are commonly applied for solving Eq. (6).

Comparing Eq. 1 with the following observation $P^+ = B(PB)^+$ shows that filtering with

$$F = (PB)^+ \quad (7)$$

in the generalized FBP formula (1) yields the same result x^\dagger as applying the generalized inverse P^+ to the measured data y .

Computation of filter kernels The computation of the filter kernels for the generalized filtered back-projection algorithm given by Eq. (1) and Eq. (7) will be demonstrated in the following for a digital breast tomosynthesis geometry. The acquisition geometry is defined by a static detector and an X-ray source moving on a straight line at fixed height above the detector parallel to its columns, see Fig. 1 (a). Therefore, each detector column consisting of M detector elements can be processed separately. However, the computation of the filter F for one particular column still requires the evaluation of the generalized inverse $(PB)^+$ of the matrix

$$PB = \begin{pmatrix} P_1 B_1 & \dots & P_1 B_N \\ \vdots & \ddots & \vdots \\ P_N B_1 & \dots & P_N B_N \end{pmatrix} , \quad (8)$$

which consists of $N \times N$ blocks of matrices of the size $M \times M$. For typical values of $M = 2048$ and $N = 17$ in digital breast tomosynthesis the numerical complexity of a direct calculation of $(PB)^+$ is $O(N^3 M^3)$ and hence too large for practical purposes.

To overcome this problem, the operator (PB) acting on the projection data is analysed in the Fourier domain. Each block matrix $P_i B_j$ describes a convolution on the projection data with a shift-invariant kernel of limited width depending on the angle between the source positions i and j , see Fig. 1 (b). Hence, the block matrices $P_i B_j$ can be described as a diagonal matrix in the frequency domain with diagonal elements given by the frequency components of the Fourier transformed convolution operator $P_i B_j$, i.e.

$$P_i \hat{B}_j = \text{diag} \left(P_i \hat{B}_j^{(1)}, \dots, P_i \hat{B}_j^{(M)} \right) , \quad (9)$$

and PB can be reordered w.r.t. the frequency components $k = 1, \dots, M$, yielding a blockdiagonal shape of M blocks of size $N \times N$ each:

$$\hat{P}B = \text{diag} \left(\hat{P}B^{(1)}, \dots, \hat{P}B^{(M)} \right) , \quad (10)$$

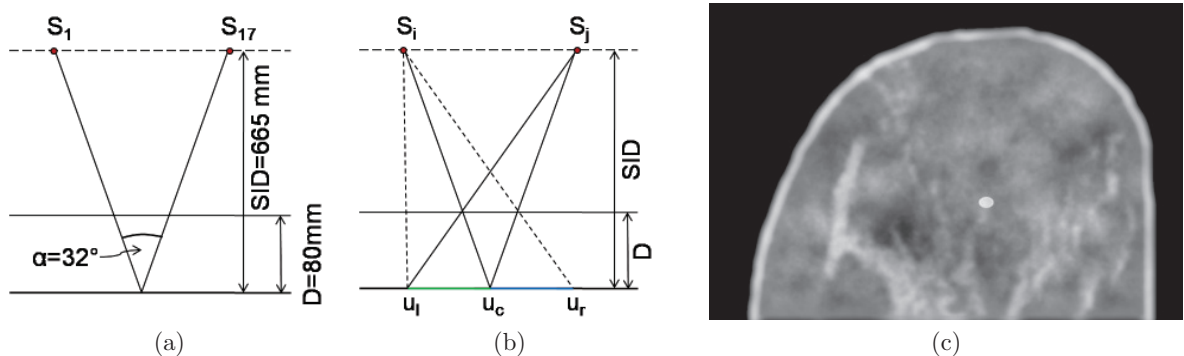


Figure 1: (a) Acquisition geometry of the simulated DBT system. (b) Illustration of shift-invariant convolution kernel of operator $P_i B_j$. (c) Axial slice through simulated breast phantom with anatomical background noise and ellipsoidal lesion.

with

$$\hat{P}B^{(k)} = \begin{pmatrix} P_1 \hat{B}_1^{(k)} & \dots & P_1 \hat{B}_N^{(k)} \\ \vdots & \ddots & \vdots \\ P_N \hat{B}_1^{(k)} & \dots & P_N \hat{B}_N^{(k)} \end{pmatrix}. \quad (11)$$

Now, the calculation of the filter $\hat{F}^{(k)} = (\hat{P}B)^{(k)+}$ can be performed separately for each frequency component $k = 1, \dots, M$, which reduces the complexity from $O(N^3 M^3)$ to $O(MN^3)$ and enables the practical implementation of the proposed method. The matrices $(\hat{P}B)^{(k)}$ can be calculated analytically for the given acquisition geometry.

Breast phantoms For this simulation study a series of breast phantoms have been generated from dynamic contrast-enhanced MRI images, acquired on a Philips MR Intera Achieva 1.5 T scanner at the University of Chicago Hospitals, by segmentation into three tissue compartments representing adipose, glandular and skin tissue and application of a compression model as previously described in [3]. To further refine these software breast phantoms, anatomic noise background structure has been added with a random signal following a power law behaviour. To this end, a random white noise signal has been Fourier transformed and multiplied with a power-law function $H(f) = B^{0.5}/f^{1.5}$ in frequency domain such that the resulting structure noise admits the power spectrum $P(f) = B/f^3$, see [1]. An exemplary breast phantom with an additional ellipsoidal lesion and a resolution of $200\ \mu\text{m}$ in each direction is depicted in Fig. 1 (c).

3 Results

Simulated projection data have been generated from breast phantoms for a DBT system with a static detector with $100\ \mu\text{m}$ pixel pitch. The tube is moving parallel to the detector columns at constant height of $SID = 665\text{ mm}$ above the detector sampling $N = 17$ projections at equidistant angles between $\pm 16^\circ$ measured against the detector normal, see Fig. 1 (a). Fig. 2 (a) - (c) show a comparison of an axial slice through the reconstructed volumes for FBP with a ramp filter, the proposed generalized FBP, and ART with 10 iterations. Fig. 2 (d) shows a profile of the attenuation values along the line indicated in the images. Obviously, standard FBP with ramp filter yields a loss of the average value and even negative values for the attenuation coefficient can occur. On the other hand, the generalized FBP and the iteratively computed ART reconstruction exhibit a very similar appearance and the line profiles shown in Fig. 2 (d) almost coincide.

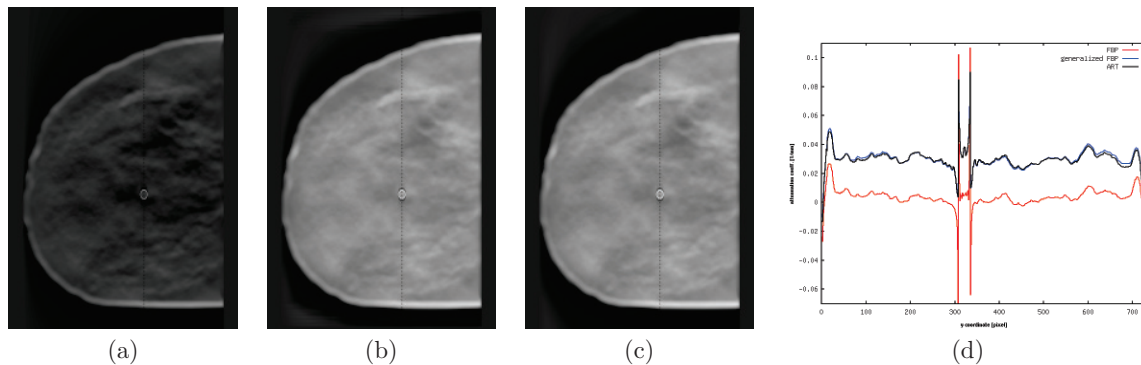


Figure 2: Axial slice reconstructions with (a) standard FBP, (b) proposed generalized FBP and (c) ART with 10 iterations. (d) shows a profiles of the reconstructed attenuation coefficient along the line indicated in (a) - (c).

4 New work to be presented

The presented filter computation method for a generalized filtered back-projection algorithm for digital breast tomosynthesis has not been presented before. To the best of our knowledge, comparable methods have not been applied to digital breast tomosynthesis before.

5 Conclusion

The proposed method yields a computationally efficient generalized FBP algorithm for digital breast tomosynthesis, which provides similar image quality as iterative reconstruction techniques while preserving the ability for region of interest reconstructions. Both a small number of views and a limited angular range can be handled with the generalized FBP while common FBP reconstruction yields a severe loss of the average value. Moreover, due to the filter computation as the pseudo-inverse operator, the reconstructed image provides an optimal solution in the least-squares sense, which minimizes the error between the measured data and the reprojections of the reconstructed image.

References

- [1] A. E. Burgess, F. L. Jacobson, and P. F. Judy. Human observer detection experiments with mammograms and power-law noise. *Med Phys*, 28(4):419–437, Apr 2001.
- [2] James T Dobbins and Devon J Godfrey. Digital x-ray tomosynthesis: current state of the art and clinical potential. *Phys Med Biol*, 48(19):R65106, Oct 2003.
- [3] Klaus Erhard, Michael Grass, and Tim Nielsen. A second pass correction method for calcification artifacts in digital breast tomosynthesis. volume 7961, page 796119. SPIE, 2011.
- [4] A. C. Kak and M. Slaney. *Principles of Computerized Tomographic Imaging*. IEEE Press, New York, 1987.